

---

---

# $^{18}\text{F}$ -FDOPA PET Imaging of Brain Tumors: Comparison Study with $^{18}\text{F}$ -FDG PET and Evaluation of Diagnostic Accuracy

Wei Chen<sup>1,2</sup>, Daniel H.S. Silverman<sup>1</sup>, Sibylle Delaloye<sup>1</sup>, Johannes Czernin<sup>1</sup>, Nirav Kamdar<sup>1</sup>, Whitney Pope<sup>3</sup>, Nagichettiar Satyamurthy<sup>1</sup>, Christiaan Schiepers<sup>1</sup>, and Timothy Cloughesy<sup>4</sup>

<sup>1</sup>Department of Molecular and Medical Pharmacology, David Geffen School of Medicine, University of California Los Angeles, Los Angeles, California; <sup>2</sup>Department of Radiology, Kaiser Permanente Woodland Hills Medical Center, Woodland Hills, California; <sup>3</sup>Department of Radiology, David Geffen School of Medicine, University of California Los Angeles, Los Angeles, California; and <sup>4</sup>Department of Neurology, David Geffen School of Medicine, University of California Los Angeles, Los Angeles, California

We evaluated the amino acid and glucose metabolism of brain tumors by using PET with 3,4-dihydroxy-6- $^{18}\text{F}$ -fluoro-L-phenylalanine ( $^{18}\text{F}$ -FDOPA) and  $^{18}\text{F}$ -FDG. **Methods:** Eighty-one patients undergoing evaluation for brain tumors were studied. Initially, 30 patients underwent PET with  $^{18}\text{F}$ -FDOPA and  $^{18}\text{F}$ -FDG within the same week. Tracer kinetics in normal brain and tumor tissues were estimated. PET uptake was quantified by use of standardized uptake values and the ratio of tumor uptake to normal hemispheric tissue uptake (T/N). In addition, PET uptake with  $^{18}\text{F}$ -FDOPA was quantified by use of ratios of tumor uptake to striatum uptake (T/S) and of tumor uptake to white matter uptake. The accuracies of  $^{18}\text{F}$ -FDOPA and  $^{18}\text{F}$ -FDG PET were determined by comparing imaging data with histologic findings and findings of clinical follow-up of up to 31 mo (mean, 20 mo). To further validate the accuracy of  $^{18}\text{F}$ -FDOPA PET,  $^{18}\text{F}$ -FDOPA PET was performed with an additional 51 patients undergoing brain tumor evaluation. **Results:** Tracer uptake in tumors on  $^{18}\text{F}$ -FDOPA scans was rapid, peaking at approximately 15 min after intravenous injection. Tumor uptake could be distinguished from that of the striatum by the difference in peak times. Both high-grade and low-grade tumors were well visualized with  $^{18}\text{F}$ -FDOPA. The sensitivity for identifying tumors was substantially higher with  $^{18}\text{F}$ -FDOPA PET than with  $^{18}\text{F}$ -FDG PET at comparable specificities, as determined by simple visual inspection, especially for the assessment of low-grade tumors. Using receiver-operating-characteristic curve analysis, we found the optimal threshold for  $^{18}\text{F}$ -FDOPA to be a T/S of greater than 1.0 (sensitivity, 96%; specificity, 100%) or a T/N of greater than 1.3 (sensitivity, 96%; specificity, 86%). The high diagnostic accuracy of  $^{18}\text{F}$ -FDOPA PET at these thresholds was confirmed with the additional 51 patients (a total of 81 patients: sensitivity, 98%; specificity, 86%; positive predictive value, 95%; negative predictive value, 95%). No significant difference in tumor uptake on  $^{18}\text{F}$ -FDOPA scans was seen between low-grade

and high-grade tumors ( $P = 0.40$ ) or between contrast-enhancing and nonenhancing tumors ( $P = 0.97$ ). Radiation necrosis was generally distinguishable from tumors on  $^{18}\text{F}$ -FDOPA scans ( $P < 0.00001$ ). **Conclusion:**  $^{18}\text{F}$ -FDOPA PET was more accurate than  $^{18}\text{F}$ -FDG PET for imaging of low-grade tumors and evaluating recurrent tumors.  $^{18}\text{F}$ -FDOPA PET may prove especially useful for imaging of recurrent low-grade tumors and for distinguishing tumor recurrence from radiation necrosis.

**Key Words:**  $^{18}\text{F}$ -FDOPA;  $^{18}\text{F}$ -FDG; PET; brain tumors; diagnosis; accuracy

**J Nucl Med 2006; 47:904–911**

**I**maging of brain tumors with  $^{18}\text{F}$ -FDG was the first oncologic application of PET (1–4). However, recent studies demonstrated its diagnostic limitations (5,6). Because of the high physiologic rate of metabolism of glucose by normal brain tissue, the detectability of tumors with only modest increases in glucose metabolism, such as low-grade tumors and, in some cases, recurrent tumors, is difficult. The best cutoff level for  $^{18}\text{F}$ -FDG uptake in the differentiation of high-grade from low-grade tumors was reported to be 1.5 for the ratio of tumor uptake to white matter uptake (T/W) (7).  $^{18}\text{F}$ -FDG uptake of low-grade tumors is usually similar to that of normal white matter, and high-grade tumor uptake can be lower than or similar to that of normal gray matter; these properties decrease the sensitivity of lesion detection. Further, there can be great variability in  $^{18}\text{F}$ -FDG uptake in that high-grade tumors may actually have uptake that is only similar to or slightly higher than white matter uptake. This is especially true in high-grade tumors after treatment (4,8). Moreover,  $^{18}\text{F}$ -FDG uptake can increase in inflammatory lesions, a property that limits the specificity of  $^{18}\text{F}$ -FDG PET for tumor detection.

Amino acid and amino acid analog PET tracers constitute another class of tumor imaging agents (9,10). They are

---

Received Nov. 7, 2005; revision accepted Feb. 11, 2006.  
For correspondence or reprints contact: Wei Chen, MD, PhD, AR-144, David Geffen School of Medicine, University of California Los Angeles, Los Angeles, CA 90095.  
E-mail: weichen@mednet.ucla.edu

particularly attractive for imaging of brain tumors because of the high uptake in tumor tissue and the low uptake in normal brain tissue. The best studied amino acid tracer is  $^{11}\text{C}$ -methionine (MET; 11). Because of the short half-life of  $^{11}\text{C}$  (20 min),  $^{18}\text{F}$ -labeled aromatic amino acid analogs have been developed for tumor imaging (12). Tumor uptake of *O*-2- $^{18}\text{F}$ -fluoroethyl-L-tyrosine and 3,4-dihydroxy-6- $^{18}\text{F}$ -fluoro-L-phenylalanine ( $^{18}\text{F}$ -FDOPA) has been reported to be similar to that of MET (13–17). Recently, the  $^{18}\text{F}$ -FDOPA metabolite 3-*O*-methyl-6- $^{18}\text{F}$ -fluoro-L-DOPA ( $^{18}\text{F}$ -OMFD) also was used for brain tumor imaging by PET (18).

This study had several aims. First, we evaluated the amino acid and glucose metabolism of primary, recurrent, or metastatic brain tumors by using PET with  $^{18}\text{F}$ -FDOPA and  $^{18}\text{F}$ -FDG. Second, using histologic and clinical follow-up findings as gold standards, we determined the diagnostic accuracies of  $^{18}\text{F}$ -FDOPA and  $^{18}\text{F}$ -FDG PET. Finally, we attempted to verify the accuracy of  $^{18}\text{F}$ -FDOPA-PET for brain tumor imaging in a larger population of patients.

## MATERIALS AND METHODS

### Patients

Initially, 30 patients with brain tumors, newly diagnosed or previously treated (18 men, 12 women; mean age  $\pm$  SD, 45.2  $\pm$  14 y; range, 23–68 y), were prospectively studied. The distribution of cases on the basis of the World Health Organization histopathologic classification was as follows: 7 patients had newly diagnosed gliomas (grade II,  $n = 3$ ; grade III,  $n = 1$ ; grade IV,  $n = 3$ ), and 23 had tumors that were previously treated by surgical resection or radiation (original primary tumors: grade II,  $n = 2$ ; grade III,  $n = 3$ ; grade IV,  $n = 15$ ; metastatic brain tumors:  $n = 3$  [breast, lung, and melanoma]). Eleven patients were being treated with corticosteroids at the time of the PET scans (dexamethasone at 1–24 mg daily; mean, 11 mg). All patients underwent  $^{18}\text{F}$ -FDOPA PET and  $^{18}\text{F}$ -FDG PET within the same week. MRI studies of the brain, including T2- and T1-weighted images, before and after the administration of gadolinium-diethylenetriaminepentaacetic acid, were acquired for all patients within 1 wk before the PET scans. The accuracies of the imaging data were validated by histologic findings (15 patients; average time to surgery, 20 d) or subsequent clinical follow-up findings (15 patients; mean follow-up time, 20 mo). For clinical follow-up, tumor progression within 6 mo after the PET study was the criterion used as clinical evidence of an aggressive tumor. Six patients died, with an average time to death of 7 mo; all had tumors that progressed within 6 mo after the PET study. The remaining 9 patients were alive at 20 mo of follow-up: 3 had radiation necrosis that was found to be resolved at follow-up MRI without treatment, 5 patients remained stable at 27 mo, and 1 patient had tumor shrinkage.

$^{18}\text{F}$ -FDOPA PET (without  $^{18}\text{F}$ -FDG PET) was subsequently expanded to a larger population of 51 patients (34 men, 17 women). There were 3 newly diagnosed gliomas (grade II,  $n = 2$ ; grade III,  $n = 1$ ), and 47 patients were evaluated for recurrence (original primary tumors: grade II,  $n = 13$ ; grade III,  $n = 13$ ; grade IV,  $n = 21$ ). One newly identified lesion was subsequently found to be benign reactive changes.

All patients gave written consent to participate in this study, which was approved by the Office for Protection of Research Subjects, University of California Los Angeles.

### $^{18}\text{F}$ -FDOPA Synthesis

$^{18}\text{F}$ -FDOPA synthesis was performed by use of a previously reported procedure (19,20). The chemical and radiochemical purities of the product isolated from the semipreparative high-pressure liquid chromatography system were further confirmed by an analytic high-pressure liquid chromatography method (specific activity,  $\sim 18.5 \times 10^{10}$  Bq/mmol [5 Ci/mmol]) and were both greater than 99%. The product was made isotonic with sodium chloride and sterilized by passage through a 0.22- $\mu\text{m}$  Millipore filter into a sterile multidose vial.

### PET Imaging

PET was performed with a high-resolution full-ring scanner (ECAT HR or ECAT HR+; Siemens/CTI), which acquired 47 or 63 contiguous slices simultaneously. For  $^{18}\text{F}$ -FDOPA PET, patients were instructed to consume a low-protein diet after the previous evening meal.  $^{18}\text{F}$ -FDOPA PET and  $^{18}\text{F}$ -FDG PET were performed in the same week for 30 patients. Patients were instructed to drink plenty of water before and after PET to accelerate renal tracer excretion.

For  $^{18}\text{F}$ -FDOPA PET, a dynamic emission acquisition sequence in the 3-dimensional mode over 75 min ( $8 \times 15$  s,  $2 \times 30$  s,  $2 \times 60$  s,  $14 \times 300$  s) was started with an intravenous injection of  $^{18}\text{F}$ -FDOPA at 3.5 MBq/kg. This dynamic acquisition was used to characterize the time-activity curve of  $^{18}\text{F}$ -FDOPA uptake and for kinetic modeling (Christiaan Schiepers et al., unpublished data, 2005). After an intravenous injection of  $^{18}\text{F}$ -FDG at 2.4 MBq/kg and after an uptake period of 60 min, static  $^{18}\text{F}$ -FDG PET images were acquired for 30 min. To minimize a patient's head motion, hypoallergenic medical tape was applied across the forehead and head cushion before the PET acquisition. To correct for photon attenuation, 5-min transmission scans were acquired after the  $^{18}\text{F}$ -FDOPA and  $^{18}\text{F}$ -FDG emission scans for all patients. PET emission data corrected for photon attenuation, photon scatter, and random coincidences were reconstructed by use of iterative reconstruction with ordered-subset expectation maximization and a gaussian filter with a full width at half maximum of 4 mm.  $^{18}\text{F}$ -FDOPA PET images were summed from 10 to 30 min after tracer injection. For  $^{18}\text{F}$ -FDG PET, one 30-min static image was obtained 60 min after tracer injection.

### Image Analysis

Standard visual image interpretation was performed independently by 2 nuclear medicine physicians for  $^{18}\text{F}$ -FDOPA PET and  $^{18}\text{F}$ -FDG PET studies with MRI as a reference. Clinical information was available to the interpreting physicians. Any tracer activities above background levels were considered abnormal for both  $^{18}\text{F}$ -FDOPA PET and  $^{18}\text{F}$ -FDG PET scans.

For semiquantitative image analysis (region of interest [ROI]), ROIs were drawn over 3 consecutive slices. Tumor ROIs were placed on the summed scans by drawing an 80% peak-voxel-intensity isocontour on the slices with maximal tumor uptake to avoid cysts and resection cavities. For tumors that did not show visible PET uptake, MRI was used as a reference through image fusion (MIM Workstation; MIMVISTA) of T1-weighted gadolinium-enhanced MR images for lesions that were contrast enhancing and T2-weighted MR images for lesions that were not contrast enhancing.

The normal reference brain region was defined by drawing an ROI involving the entire contralateral hemisphere at the level of the centrum semiovale. For the determination of tracer uptake in normal gray matter and white matter, 3 circular ROIs with 8-mm diameters were placed along the cortical band of the contralateral frontal and parietal cortices (gray matter) and in the centrum semiovale (white matter) (7). The ROIs from the frontal and parietal cortices then were averaged to generate the gray matter data. ROIs also were drawn over the contralateral striatum and the entire cerebellum.

Activity counts in the ROIs were normalized to injected dose per kilogram of patient body weight (standardized uptake value [SUV]). The peak pixel SUV ( $SUV_{max}$ ) and the mean SUV of the voxels falling within the 80% peak-voxel-intensity isocontour ( $SUV_{max20}$ ) were generated. Ratios of tumor uptake to normal tissue uptake were generated by dividing the tumor  $SUV_{max20}$  by the SUV of the contralateral normal hemispheric brain tissue (T/N), the normal striatum (T/S), and the normal white matter (T/W).

To determine the time course of tracer uptake in tumor ROIs and the time to reach the optimal ratio of tumor activity to background activity, time-activity curves over the entire acquisition period were generated. ROIs were copied to dynamic  $^{18}F$ -FDOPA PET image sets. Uptake curves for the tumor, cerebellum (as the blood-pool reference), normal gray and white matter, and the striatum were generated over the 75 min after injection.

### Statistical Analysis

$^{18}F$ -FDG and  $^{18}F$ -FDOPA PET scan parameters were compared by use of the Wilcoxon nonparametric test. The Student *t* test was used to compare the  $^{18}F$ -FDG and  $^{18}F$ -FDOPA SUVs of high-grade versus low-grade tumors, contrast-enhancing versus non-enhancing tumors, and tumors versus radiation necrosis. Sensitivity and specificity were calculated by comparing the PET data with histologic and clinical follow-up data. Data are presented with 95% confidence intervals (CIs). Receiver-operating-characteristic (ROC) curve analysis for the first group of 30 patients undergoing  $^{18}F$ -FDOPA PET was used to determine the optimal thresholds for the uptake ratios (T/N, T/S, and T/W). The optimal thresholds identified then were applied and tested with the second  $^{18}F$ -FDOPA study patient population ( $n = 51$ ) as well as with the entire population (the first and second groups of patients together;  $n = 81$ ).

## RESULTS

### Time-Activity Curves for $^{18}F$ -FDOPA PET Scans

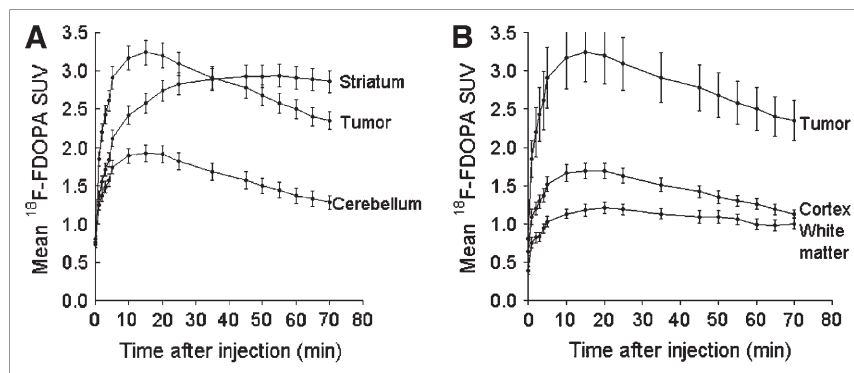
Representative decay-corrected time-activity curves for the tumor, the cerebellum, and the striatum were averaged

over the first 11 patients undergoing  $^{18}F$ -FDOPA PET (Fig. 1A). This information was used in this study to select the time window for obtaining the highest tumor uptake while maintaining a good ratio of tumor uptake to normal tissue uptake. The highest tracer uptake in the tumor and cerebellum generally occurred between 10 min and 30 min after injection. SUVs (mean  $\pm$  SD) were  $3.24 \pm 0.39$  at 15 min. Mean tumor uptake reached 98% of peak activity (SUV,  $3.17 \pm 0.41$ ) at 10 min and still averaged 93% of peak activity (SUV,  $3.00 \pm 0.30$ ) at 30 min. There was no difference in time-activity curve patterns between high-grade and low-grade tumors. The cerebellum had lower uptake than tumor (peak SUV,  $1.92 \pm 0.11$ ). At the end of the study at 75 min, tumor uptake had declined to 73% of its peak activity (SUV,  $2.35 \pm 0.26$ ), and cerebellar uptake had declined to 67% of its peak activity (SUV,  $1.28 \pm 0.09$ ). Tracer activity in the striatum did not reach a peak until 50 min after injection (SUV,  $2.93 \pm 0.70$ ), and there was no significant decline at 75 min after injection (SUV,  $2.86 \pm 0.70$ ; 98% peak activity). Thus, tumor uptake from 10–30 min after injection is nearly maximal and occurs sufficiently early to avoid peak uptake in the striatum. SUVs were higher in normal gray matter (SUV,  $1.69 \pm 0.11$ ) than in normal white matter (SUV,  $1.21 \pm 0.07$ ) ( $P = 0.0001$ ) (Fig. 1B). Gray matter uptake declined to 67% of peak activity at 75 min, whereas white matter uptake declined to 83% of peak activity at 75 min.

### Visual Image Analysis

With the criterion that any tracer activity above the background should be considered abnormal, 22 of 23 high-grade and low-grade tumors were visualized by  $^{18}F$ -FDOPA PET (Fig. 2); there was 1 false-negative result in a patient with a residual low-grade tumor. All 3 patients without active disease (in long-term remission) lacked any visible uptake on  $^{18}F$ -FDOPA PET scans. Four patients with radiation necrosis had very low but visible  $^{18}F$ -FDOPA uptake. Thus,  $^{18}F$ -FDOPA had a sensitivity of 96%, a specificity of 43%, and an overall accuracy of 83% (95% CI, 70%–97%). These data corresponded to a positive predictive value (PPV) of 85% and a negative predictive value (NPV) of 75% (Table 1).

**FIGURE 1.** Time-activity curves for tracer uptake on  $^{18}F$ -FDOPA PET scans summarized for 11 patients over 75 min from time of injection. (A) Time course of tracer accumulation in tumor tissue, cerebellum, and striatum. Tumor uptake is expressed as mean values of voxels with top 20% SUVs. Error bars denote 1 SE from mean uptake. (B) Time course of tracer accumulation in tumor tissue, cortex, and white matter. Error bars denote 1 SE from mean uptake.



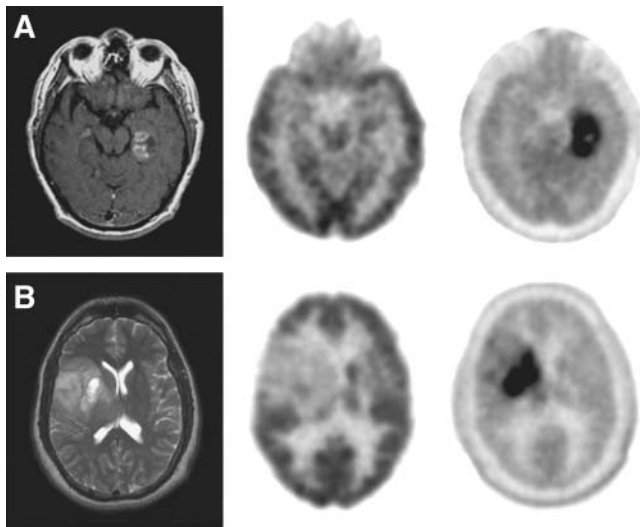


**FIGURE 2.** MRI (left),  $^{18}\text{F}$ -FDG PET (middle), and  $^{18}\text{F}$ -FDOPA PET (right) of newly diagnosed tumors. (A) Glioblastoma. (B) Grade II oligodendroglioma.

Using the same visual criterion, 14 of 23 tumors were visualized by  $^{18}\text{F}$ -FDG PET (sensitivity, 61%) (Table 1). Eight of the 9 tumors that were negative on  $^{18}\text{F}$ -FDG scans were clearly visible on  $^{18}\text{F}$ -FDOPA scans (Fig. 3). One of these patients had had a grade II oligodendroglioma resected 5 y before and began experiencing seizures.  $^{18}\text{F}$ -FDOPA PET demonstrated the recurrent tumor, which was subsequently localized by intraoperative electroencephalography and resected (Fig. 3B). The other 7 patients suffered tumor progression within 1–3 mo after the PET study. Similar to the results obtained for  $^{18}\text{F}$ -FDOPA uptake, there was no visible  $^{18}\text{F}$ -FDG uptake in 3 stable patients in long-term remission, and there was low-level  $^{18}\text{F}$ -FDG uptake in 4 patients with radiation necrosis (specificity, 43%). These data corresponded to a PPV for  $^{18}\text{F}$ -FDG of 78%, an NPV of 25%, and an overall accuracy of 57% (95% CI, 39%–74%). Thus,  $^{18}\text{F}$ -FDOPA PET was more sensitive (sensitivity, 96%; 95% CI, 87%–100%) in identifying tumors

**TABLE 1**  
Sensitivity and Specificity of  $^{18}\text{F}$ -FDOPA and  $^{18}\text{F}$ -FDG,  
as Determined by Simple Visual Analysis

Comparison	Histopathology or clinical follow-up	
	Positive	Negative
$^{18}\text{F}$ -FDOPA positive	22	4
$^{18}\text{F}$ -FDOPA negative	1	3
$^{18}\text{F}$ -FDG positive	14	4
$^{18}\text{F}$ -FDG negative	9	3

For  $^{18}\text{F}$ -FDOPA, sensitivity was 96%, specificity was 43%, PPV was 85%, and NPV was 75%. For  $^{18}\text{F}$ -FDG, sensitivity was 61%, specificity was 43%, PPV was 78%, and NPV was 25%.

overall than  $^{18}\text{F}$ -FDG PET (sensitivity, 61%; 95% CI, 41%–81%).

Four patients were evaluated for radiation necrosis suspected by clinical assessment (3 with metastatic cancers: breast, lung, and melanoma; 1 with grade III glioma). Three of these patients were determined to have radiation necrosis on the basis of the observation of spontaneous regression of contrast-enhanced lesions in the subsequent months without treatment; 1 was found to have a recurrent tumor (breast cancer) on the basis of biopsy and was subsequently treated.  $^{18}\text{F}$ -FDOPA correctly identified the recurrent tumor, and  $^{18}\text{F}$ -FDG yielded false-negative results.

#### Comparison of $^{18}\text{F}$ -FDOPA and $^{18}\text{F}$ -FDG PET Scans for High-Grade and Low-Grade Tumors

For the 23 confirmed tumors,  $^{18}\text{F}$ -FDOPA had an  $\text{SUV}_{\text{max}}$  of  $4.39 \pm 2.10$  and a T/N of  $2.50 \pm 0.73$  for high-grade tumors ( $n = 18$ ) and an  $\text{SUV}_{\text{max}}$  of  $3.07 \pm 1.65$  and a T/N of  $1.95 \pm 0.69$  for low-grade tumors ( $n = 5$ ) (Table 2). The 7 patients with changes after treatment had an  $\text{SUV}_{\text{max}}$  of  $1.50 \pm 0.35$  and a T/N of  $1.11 \pm 0.25$ . Among these 7 patients, the 4 radiation necrosis lesions had an  $\text{SUV}_{\text{max}}$  of  $1.57 \pm 0.47$  and a T/N of  $1.25 \pm 0.23$ .

$^{18}\text{F}$ -FDG had higher absolute SUVs than  $^{18}\text{F}$ -FDOPA, with  $\text{SUV}_{\text{max}}$  values of  $5.49 \pm 3.16$  and  $2.48 \pm 0.85$  for the 19 high-grade and 5 low-grade tumors. However, the T/N values of  $^{18}\text{F}$ -FDG were  $1.23 \pm 0.69$  for high-grade tumors and  $0.66 \pm 0.33$  for low-grade tumors. Thus, the contrast for imaging of tumors was higher with  $^{18}\text{F}$ -FDOPA. The difference between  $^{18}\text{F}$ -FDOPA and  $^{18}\text{F}$ -FDG T/N values was statistically significant ( $P < 0.001$ ).

#### ROC Analysis of $^{18}\text{F}$ -FDOPA Sensitivity and Specificity

As described above, standard visual analysis of  $^{18}\text{F}$ -FDOPA PET seemed adequate in that it provided a high sensitivity for identifying tumors. However, the specificity

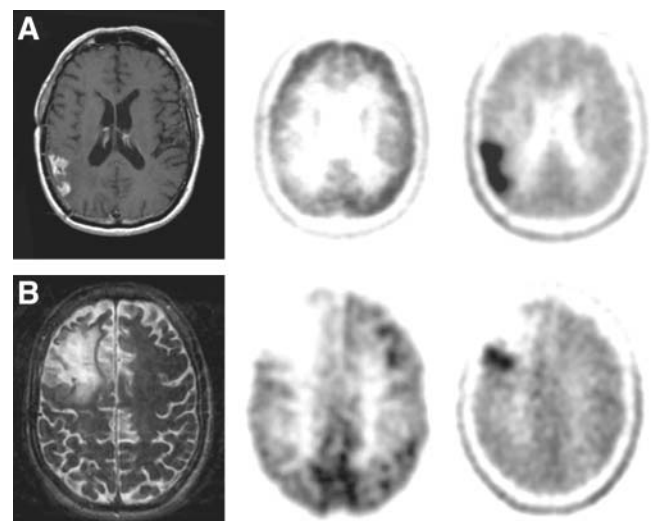


**FIGURE 3.** MRI (left),  $^{18}\text{F}$ -FDG PET (middle), and  $^{18}\text{F}$ -FDOPA PET (right) for evaluating recurrent tumors. (A) Recurrent glioblastoma. (B) Recurrent grade II oligodendroglioma.

**TABLE 2**  
<sup>18</sup>F-FDOPA and <sup>18</sup>F-FDG Parameters in High-Grade and Low-Grade Tumors and Post-Treatment Changes

Tumor grade or post-treatment changes (no. of tumors)	<sup>18</sup> F-FDOPA		<sup>18</sup> F-FDG	
	SUV <sub>max</sub>	T/N	SUV <sub>max</sub>	T/N
High grade ( <i>n</i> = 18)	4.39 ± 2.10	2.50 ± 0.73	5.49 ± 3.16	1.23 ± 0.69
Low grade ( <i>n</i> = 5)	3.07 ± 1.65	1.95 ± 0.69	2.48 ± 0.85	0.66 ± 0.33
Post-treatment changes ( <i>n</i> = 7)	1.50 ± 0.35	1.11 ± 0.25	3.13 ± 1.27	0.74 ± 0.09

Data are reported as mean ± SD.

was low, as radiation necrosis lesions all had low but visible tracer uptake. Therefore, ROC analysis was used to identify the optimal thresholds for various ratios of tumor uptake to normal tissue uptake: T/N, T/S, and T/W.

A T/S of 0.75 or 1.0, a T/N of 1.3, and a T/W of 1.6 were found to provide the best sensitivity and specificity (Table 3). A T/S of 0.75 provided a sensitivity of 100% and a specificity of 86%, a T/S of 1.0 provided a sensitivity of 96% and a specificity of 100%, a T/N of 1.3 provided a sensitivity of 96% and a specificity of 86%, and a T/W of 1.6 provided a sensitivity of 96% and a specificity of 86%.

**Prospective Application of Thresholds to Larger Patient Population**

An additional 51 patients were studied by <sup>18</sup>F-FDOPA PET to test the thresholds for sensitivity and specificity generated from the ROC analysis of the first group of 30 patients studied. This second group of patients included more post-treatment patients being monitored for disease status (*n* = 47) (Table 4). <sup>18</sup>F-FDOPA data were compared with pathology findings (10 patients; mean time to surgery: 25 d) and clinical follow-up findings (41 patients; mean follow-up time: 11 mo). Fourteen patients died during the follow-up period, with the mean time to death of 4.5 mo.

A T/S of 0.75 or 1.0, a T/N of 1.3, and a T/W of 1.6 were used in this group of patients to evaluate sensitivity, specificity, PPV, and NPV (Table 5). As shown in Table 5, a T/S of 0.75 provided a similar sensitivity (97% vs. 100%) and the same specificity (86%) for the second group of patients as for the first group of patients. Likewise, a T/N of 1.3 provided a similar sensitivity (95% vs. 96%) and the same specificity (86%) for the second group of patients as for the first group of patients. When the 2 groups of patients were

considered together (*n* = 81), a T/S of 0.75 and a T/N of 1.3 again yielded the best diagnostic accuracy (T/S of 0.75: sensitivity, 98%; specificity, 86%; PPV, 95%; NPV, 95%; accuracy, 95%; T/N of 1.3: sensitivity, 95%; specificity, 86%; PPV, 95%; NPV, 86%; accuracy, 93%).

There was no statistically significant difference between uptake levels in 48 high-grade tumors and 18 low-grade tumors (*P* = 0.40) (Fig. 4A). Furthermore, contrast-enhancing tumors (*n* = 37) and nonenhancing tumors (*n* = 23) had similar SUV<sub>max</sub> values (3.57 ± 1.74 versus 2.88 ± 1.14) (*P* = 0.97) (Fig. 4B), supporting the notion that a blood-brain barrier breakdown is not a prerequisite for uptake into tumors. There was a statistically significant difference in uptake levels between contrast-enhancing tumors and radiation necrosis lesions (*n* = 4) (*P* < 0.00001).

**DISCUSSION**

To our knowledge, this is the first clinical study to systematically compare <sup>18</sup>F-FDOPA PET with <sup>18</sup>F-FDG PET of brain tumors and to evaluate the diagnostic accuracy of <sup>18</sup>F-FDOPA PET for a relatively large number of patients with pathologic and clinical follow-up findings. Our results suggest that <sup>18</sup>F-FDOPA PET is superior to <sup>18</sup>F-FDG PET

**TABLE 4**  
Clinical Characteristics of Group 1 and Group 2 Patients

Clinical disease status	Group 1 patients ( <i>n</i> = 30)	Group 2 patients ( <i>n</i> = 51)	Combining 2 groups ( <i>n</i> = 81)
Newly diagnosed patients			
Grade II	3	2	5
Grade III	1	1	2
Grade IV	3	0	3
Nontumor	0	1	1
Clinically stable patients			
Grade II	2	6	8
Grade III	1	7	8
Grade IV	6	5	11
Post-treatment patients			
Recurrent: Grade II	1	4	5
Grade III	2	1	3
Grade IV	5	15	20
Post-treatment changes	3	8	11
Long-term remission	3	1	4

**TABLE 3**

ROC Analysis of 30 <sup>18</sup>F-FDOPA PET Studies to Generate Optimal Thresholds for Sensitivity and Specificity

Ratio	% Sensitivity (95% CI)	% Specificity (95% CI)	% PPV	% NPV
T/S > 1.0	96 (87–100)	100 (100–100)	100	88
T/S > 0.75	100 (100–100)	86 (60–100)	96	100
T/N > 1.3	96 (87–100)	86 (60–100)	96	86
T/W > 1.6	96 (87–100)	86 (60–100)	96	86

**TABLE 5**

Diagnostic Accuracy of  $^{18}\text{F}$ -FDOPA PET at Various Thresholds for Ratios of Tumor Uptake to Normal Tissue Uptake in Group 1 and Group 2 Patients

Threshold for ratio of tumor uptake to normal tissue uptake	Parameter (%)	Group 1 patients (n = 30)	Group 2 patients (n = 51)	Combining 2 groups (n = 81)
T/S > 0.75	Sensitivity	100	97	98
	Specificity	86	86	86
	Accuracy	97	94	95
	PPV	96	95	95
	NPV	100	92	95
T/S > 1.0	Sensitivity	96	86	92
	Specificity	100	93	95
	Accuracy	97	88	93
	PPV	100	94	98
	NPV	88	75	80
T/N > 1.3	Sensitivity	96	95	95
	Specificity	86	86	86
	Accuracy	93	94	93
	PPV	96	95	95
	NPV	86	92	86
T/W > 1.6	Sensitivity	96	92	93
	Specificity	86	86	86
	Accuracy	93	84	91
	PPV	96	87	95
	NPV	86	75	82

for visualizing low-grade tumors, evaluating recurrent tumors, and differentiating tumor recurrence from radiation necrosis.

$^{18}\text{F}$ -FDOPA PET of gliomas demonstrated lower SUVs than did  $^{18}\text{F}$ -FDG PET. However, the contrast between tumor tissue and normal tissue was higher with  $^{18}\text{F}$ -FDOPA than with  $^{18}\text{F}$ -FDG because of the low normal brain tissue uptake in  $^{18}\text{F}$ -FDOPA PET scans. This property proved useful in detecting low-grade tumors as well as recurrent tumors. For example, 8 of 9 patients with recurrent tumors had negative  $^{18}\text{F}$ -FDG PET results but positive  $^{18}\text{F}$ -FDOPA

PET results. Of these 9 patients, 5 had low-grade tumors and 4 had high-grade tumors. If only high-grade tumors were considered, then  $^{18}\text{F}$ -FDG sensitivity for detecting recurrent tumors would be 78% (14/18) rather than 61% (14/23), compared with 96% (22/23) for  $^{18}\text{F}$ -FDOPA. Eleven of 30 patients were receiving various doses of dexamethasone at the time of  $^{18}\text{F}$ -FDG PET. This treatment could very well decrease  $^{18}\text{F}$ -FDG uptake (21). However, because steroids are commonly used in clinical settings, this finding further indicates the difficulty of using  $^{18}\text{F}$ -FDG for brain tumor patients.  $^{18}\text{F}$ -FDOPA PET therefore may help to detect low-grade and recurrent tumors with greater sensitivity than  $^{18}\text{F}$ -FDG PET.

It was shown previously that  $^{18}\text{F}$ -FDG SUVs in brain tumors were not a reliable measure for grading or evaluating recurrent tumors (22); we obtained similar findings in the present study. In addition, it was also shown that there was an overlap of  $^{18}\text{F}$ -FDG uptake in recurrent tumors and radiation necrosis, in that even high-grade recurrent tumors could have uptake similar to or slightly above that of white matter and that necrosis could have uptake higher than that of normal white matter (5,6). In the present study, standard visual inspection of images with the criterion that any uptake above the background should be considered abnormal provided a higher sensitivity with  $^{18}\text{F}$ -FDOPA PET than with  $^{18}\text{F}$ -FDG PET. However, the specificity of  $^{18}\text{F}$ -FDOPA PET was as poor as that of  $^{18}\text{F}$ -FDG PET with the visual criterion.

We used ROC analysis to identify optimal ratios of tumor uptake to normal tissue uptake that would give the best sensitivity and specificity for  $^{18}\text{F}$ -FDOPA and applied these thresholds to a second, larger group of patients. Our results showed that the specificity of  $^{18}\text{F}$ -FDOPA brain tumor imaging could be greatly increased by using the following thresholds: T/S of 0.75 or 1.0, T/N of 1.3, and T/W of 1.6.

Although a T/S of 0.75 resulted in a slightly higher accuracy of 95% and a sensitivity of 98%, a ratio of 1.0 provided a slightly lower sensitivity of 92% but a higher specificity of 95%. The latter is clinically more practical, as

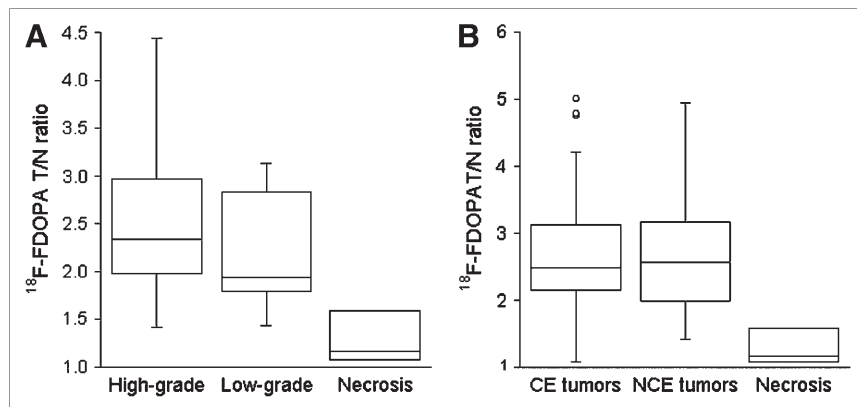


**FIGURE 4.** (A) Box plots of  $^{18}\text{F}$ -FDOPA T/N values in high-grade and low-grade brain tumors and radiation necrosis. There was no statistically significant difference between high-grade and low-grade tumors ( $P = 0.40$ ). There was a statistically significant difference between tumors and radiation necrosis ( $P < 0.00001$ ). Error bars indicate SEs. (B) Box plots of  $^{18}\text{F}$ -FDOPA T/N values in brain tumors that were contrast

enhancing on MRI (CE) and those that did not take up contrast material on MRI (NCE). No statistical difference was seen between CE and NCE tumors ( $P = 0.40$ ). Statistically significant difference was seen between CE tumors and radiation necrosis ( $P < 0.00001$ ). Error bars indicate SEs.

it does not require quantitative measurement, is visually more obvious, and is still highly accurate (accuracy, 93%; PPV, 98%; NPV, 80%). We therefore suggest the use of a T/S of 1.0 as a first-line assessment tool and the use of a T/S of 0.75 in inconclusive cases. In addition, a T/S of 1.0 could be used when there is a higher clinical suspicion of radiation necrosis, and a T/S of 0.75 could be used when there is a higher clinical suspicion of recurrent tumor.

Tumor grade did not significantly affect tracer uptake in 81 lesions in our  $^{18}\text{F}$ -FDOPA PET studies, a finding that is consistent with the results of most studies with amino acid tracers (14,17,18). Likewise, no statistically significant difference in uptake levels between tumors that were contrast enhancing and those that were nonenhancing was seen, in agreement with the notion that, like the tumor accumulation of other amino acid tracers, the tumor accumulation of  $^{18}\text{F}$ -FDOPA most likely is mediated through a specific transport system rather than requiring the breakdown of the blood-brain barrier (23).

$^{18}\text{F}$ -FDOPA has been used in evaluating patients with movement disorders for many years through imaging of the integrity of the striatal dopamine pathway (24–26). However,  $^{18}\text{F}$ -FDOPA is also an amino acid analog and was shown to be taken up at the blood-brain barrier in normal brain by the neutral amino acid transporter (27,28). Although the mechanism of tumor-specific  $^{18}\text{F}$ -FDOPA uptake has not been firmly established, other amino acid tracers, including a closely related metabolite of  $^{18}\text{F}$ -FDOPA,  $^{18}\text{F}$ -OMFD, as well as  $O$ -2- $^{18}\text{F}$ -fluoroethyl-L-tyrosine and  $^{11}\text{C}$ -methionine, have been shown to be taken up by tumors through the neutral amino acid transporter (29–33). In the present study, tumor uptake most likely included a combination of  $^{18}\text{F}$ -FDOPA and its metabolite  $^{18}\text{F}$ -OMFD, as  $^{18}\text{F}$ -OMFD uptake in brain tumors has been demonstrated to have a similar kinetic profile and to achieve a similar ratio of tumor uptake to normal tissue uptake (18). Carbidopa was not considered necessary for the clinical purpose studied here, because both  $^{18}\text{F}$ -OMFD and  $^{18}\text{F}$ -FDOPA most likely are taken up by tumors in similar ways.

A highly significant difference was seen between contrast-enhancing tumors and radiation necrosis on  $^{18}\text{F}$ -FDOPA PET scans. Larger studies would be helpful to further address the usefulness of  $^{18}\text{F}$ -FDOPA PET in distinguishing between recurrent tumors and radiation necrosis.

## CONCLUSION

$^{18}\text{F}$ -FDOPA PET demonstrated excellent visualization of high-grade and low-grade tumors. It was more sensitive and specific for evaluating recurrent tumors than was  $^{18}\text{F}$ -FDG PET. It may prove particularly valuable for examining recurrent low-grade gliomas, because these tumors are difficult to evaluate by MRI and are usually not visible on  $^{18}\text{F}$ -FDG PET scans. Our data also suggest that  $^{18}\text{F}$ -FDOPA may be valuable for distinguishing recurrent tumors from radiation necrosis, although a larger series of radiation necrosis cases is needed to confirm this suggestion.

## ACKNOWLEDGMENTS

The authors thank Amber Luke for administrative support, Michael Quinn for MRI database support, the University of California Los Angeles Cyclotron staff for PET tracer production, and University of California Los Angeles Ahmanson Biological Imaging Center technologists Larry Pang and Jean-Richard Eugene for their support in PET acquisition. This study was supported by grant P50 CA086306 from the National Cancer Institute, National Institute of Health, and by U.S. Department of Energy contract DE-FC03-87-ER60615.

## REFERENCES

1. Patronas NJ, Di Chiro G, Brooks RA, et al. Work in progress: [ $^{18}\text{F}$ ]fluorodeoxyglucose and positron emission tomography in the evaluation of radiation necrosis of the brain. *Radiology*. 1982;144:885–889.
2. Di Chiro G, Oldfield E, Wright DC, et al. Cerebral necrosis after radiotherapy and/or intraarterial chemotherapy for brain tumors: PET and neuropathologic studies. *AJR*. 1988;150:189–197.
3. Doyle WK, Budinger TF, Valk PE, Levin VA, Gutin PH. Differentiation of cerebral radiation necrosis from tumor recurrence by [ $^{18}\text{F}$ ]FDG and  $^{82}\text{Rb}$  positron emission tomography. *J Comput Assist Tomogr*. 1987;11:563–570.
4. Wong TZ, van der Westhuizen GJ, Coleman RE. Positron emission tomography imaging of brain tumors. *Neuroimaging Clin N Am*. 2002;12:615–626.
5. Olivero WC, Dulebohn SC, Lister JR. The use of PET in evaluating patients with primary brain tumors: Is it useful? *J Neurol Neurosurg Psychiatry*. 1995;58:250–252.
6. Ricci PE, Karis JP, Heiserman JE, et al. Differentiating recurrent tumor from radiation necrosis: time for re-evaluation of positron emission tomography? *Am J Neuroradiol*. 1998;19:407–413.
7. Delbecq D, Meyerowitz C, Lapidus RL, et al. Optimal cutoff levels of F-18 fluorodeoxyglucose uptake in the differentiation of low-grade from high-grade brain tumors with PET. *Radiology*. 1995;195:47–52.
8. Padoma MV, Said S, Jacobs M, et al. Prediction of pathology and survival by FDG PET in gliomas. *J Neurooncol*. 2003;64:227–237.
9. Ishiwata K, Kutota K, Murakami M, et al. Reevaluation of amino acid PET studies: Can the protein synthesis rates in brain and tumor tissues be measured in vivo? *J Nucl Med*. 1993;34:1936–1943.
10. Jager PL, Vaalburg W, Pruijm J, et al. Radiolabeled amino acids: basic aspects and clinical applications in oncology. *J Nucl Med*. 2001;42:432–445.
11. Herholz K, Holzer T, Bauer B, et al.  $^{11}\text{C}$ -Methionine PET for differential diagnosis of low-grade gliomas. *Neurology*. 1998;50:1316–1322.
12. Laverman P, Boerman OC, Corstens FHM, et al. Fluorinated amino acids for tumour imaging with positron emission tomography. *Eur J Nucl Med*. 2002;29:681–690.
13. Wester HJ, Herz M, Weber W, et al. Synthesis and radiopharmacology of  $O$ -(2-[ $^{18}\text{F}$ ]fluoroethyl)-L-tyrosine for tumor imaging. *J Nucl Med*. 1999;40:205–212.
14. Weber WA, Wester HJ, Grosu AL, et al.  $O$ -(2-[ $^{18}\text{F}$ ]fluoroethyl)-L-tyrosine and L-[methyl- $^{11}\text{C}$ ]methionine uptake in brain tumours: initial results of a comparative study. *Eur J Nucl Med*. 2000;27:542–549.
15. Pauleit D, Floeth F, Hamacher K, et al.  $O$ -(2-[ $^{18}\text{F}$ ]fluoroethyl)-L-tyrosine PET combined with MRI improves the diagnostic assessment of cerebral gliomas. *Brain*. 2005;128:678–687.
16. Heiss WD, Wienhard K, Wagner R, et al. F-Dopa as an amino acid tracer to detect brain tumors. *J Nucl Med*. 1996;37:1180–1182.
17. Becherer A, Karanikas G, Szabo M, et al. Brain tumour imaging with PET: a comparison between [ $^{18}\text{F}$ ]fluorodopa and [ $^{11}\text{C}$ ]methionine. *Eur J Nucl Med Mol Imaging*. 2003;30:1561–1567.
18. Beuthien-Baumann B, Bredow J, Burchert W, et al. 3- $O$ -Methyl-6-[ $^{18}\text{F}$ ]fluoro-L-DOPA and its evaluation in brain tumour imaging. *Eur J Nucl Med Mol Imaging*. 2003;30:1004–1008.
19. Namavari M, Bishop A, Satyamurthy N, Bida G, Barrio JR. Regioselective radiofluorodestannylation with [ $^{18}\text{F}$ ]F $_2$  and [ $^{18}\text{F}$ ]CH $_3$ COOF: a high yield synthesis of 6-[ $^{18}\text{F}$ ]fluor-L-dopa. *Appl Radiat Isot*. 1992;43:989–996.
20. Bishop A, Satyamurthy N, Bida G, Hendry G, Phelps M, Barrio JR. Proton irradiation of [ $^{18}\text{O}$ ]O $_2$ : production of [ $^{18}\text{F}$ ]F $_2$  and [ $^{18}\text{F}$ ]F $_2$  + [ $^{18}\text{F}$ ]OF $_2$ . *Nucl Med Biol*. 1996;23:189–199.

21. Fulham MJ, Brunetti A, Aloj L, Raman R, Dwyer AJ, Di Chiro G. Decreased cerebral glucose metabolism in patients with brain tumors: an effect of corticosteroids. *J Neurosurg.* 1995;83:657–664.
22. Hustinx R, Smith RJ, Benard F, Bhatnagar A, Alavi A. Can the standardized uptake value characterize primary brain tumors on FDG-PET? *Eur J Nucl Med.* 1999;26:1501–1509.
23. Oldendorf WH, Szabo J. Amino acid assignment to one of the three blood-brain barrier amino acid carriers. *Am J Physiol.* 1976;230:94–98.
24. Garnett S, Firnau G, Nahmias C, Chirakal R. Striatal dopamine metabolism in living monkeys examined by positron emission tomography. *Brain Res.* 1983;280:169–171.
25. Garnett ES, Firnau G, Nahmias C. Dopamine visualized in the basal ganglia of living man. *Nature.* 1983;305:137–138.
26. Herholz K, Heiss WD. Positron emission tomography in clinical neurology. *Mol Imaging Biol.* 2004;6:239–269.
27. Yee RE, Cheng DW, Huang SC, et al. Blood-brain barrier and neuronal membrane transport of 6-[<sup>18</sup>F]fluoro-L-DOPA. *Biochem Pharmacol.* 2001;62:1409–1415.
28. Stout DB, Huang SC, Melega WP, et al. Effects of large neutral amino acid concentrations on 6-[F-18]fluoro-L-DOPA kinetics. *J Cereb Blood Flow Metab.* 1998;18:43–51.
29. Langen KJ, Ziemons K, Kiwit JC, et al. 3-[<sup>123</sup>I]Iodo-alpha-methyltyrosine and [methyl-<sup>11</sup>C]-L-methionine uptake in cerebral gliomas: a comparative study using SPECT and PET. *J Nucl Med.* 1997;38:517–522.
30. O'Tuama LA, Guilarte TR, Douglass KH, et al. Assessment of [<sup>11</sup>C]-L-methionine transport into the human brain. *J Cereb Blood Flow Metab.* 1988;8:341–345.
31. Langen KJ, Clauss RP, Holschbach M, et al. Comparison of iodotyrosines and methionine uptake in a rat glioma model. *J Nucl Med.* 1998;39:1596–1599.
32. Langen KJ, Jarosch M, Muhlensiepen H, et al. Comparison of fluorotyrosines and methionine uptake in F98 rat gliomas. *Nucl Med Biol.* 2003;30:501–508.
33. Bergmann R, Pietzsch J, Fuechtner F, et al. 3-O-Methyl-6-<sup>18</sup>F-fluoro-L-dopa, a new tumor imaging agent: investigation of transport mechanism in vitro. *J Nucl Med.* 2004;45:2116–2122.